Ab Initio MO Analysis of Interaction Paths between Radicals in Ferromagnetic Organic Systems

Yuuichi Orimoto,[†] Takahiro Imai,[‡] Kazunari Naka,[‡] and Yuriko Aoki*[,†,§]

Department of Material Sciences, Faculty of Engineering Sciences, Kyushu University, 6-1 Kasuga-Park, Fukuoka 816-8580, Japan, Department of Chemistry, Graduate School of Science, Hiroshima University, 1-3-1 Kagamiyama, Higashi-Hiroshima 739-8526, Japan, and Group, PRESTO, Japan Science and Technology Agency (JST), Kawaguchi Center Building, 4-1-8 Honcho, Kawaguchi, Saitama 332-0012, Japan

Received: January 23, 2006; In Final Form: March 5, 2006

Interaction path analyses for π-conjugated organic systems were performed at the ab initio molecular orbital level to examine the relationship between inter-radical interactions and the high-spin stability of the system. It was found that the high-spin stability results from through-bond interactions between radicals, not from through-space interactions, in relation to the stabilization of a low-spin state due to the effects of electron correlation. $L_{ij}^{\min}$ value for estimating the mixing of nonbonding molecular orbitals well predicted the relationship between the through-bond interactions and the high-spin stability. Furthermore, molecular orbital calculations revealed that the all-trans type interaction path between radicals produces long-range exchange interactions, and the additivity of high-spin stability is observed by keeping short-range through-bond interaction paths.

Introduction

Recently, numerous attempts have been made to synthesize organic systems with ferromagnetic properties. Syntheses of crystalline solids involving small radical molecules play important roles in these studies.[1,2] However, the transition temperature of such systems is considerably low because through-space interactions between radical molecules produce very weak exchange interactions. In contrast, π-conjugated radical systems have been the subject of chemists as an alternative approach to the study of ferromagnetic organic systems.[3−10] This is because a high-transition temperature was theoretically predicted for such conjugated systems due to the strong exchange interactions between radicals through bonds.[11] Rajca et al. actually succeeded in synthesizing ultrahigh-spin π-conjugated systems in which the spin quantum number (S) is more than 5000.[10]

A large number of studies have been performed to elucidate the ferromagnetism in π-conjugated systems both experimentally[12−17] and theoretically.[18−23] With a theoretical theme, Borden et al. conducted a molecular orbital (MO) approach to the relationship between exchange interactions and ferromagnetism in conjugated systems.[24−26] In another MO approach to ferromagnetisms, one of the authors, Aoki et al., proposed a simple rule to predict high-spin stabilities of π-conjugated systems.[27] They emphasized (see ref 27) that for alternant hydrocarbon systems the 0-$*$ combination between radical units is effective for designing high-spin polymers, where "0" denotes an inactive carbon atom with no coefficients and "$*$" denotes an active carbon atom with MO coefficients in nonbonding molecular orbitals (NBMOs). The 0-$*$ type combination results in a "nondisjoint type" linkage in the system, and the linkage provides a mixing between NBMOs with their energy levels unchanged, which is closely related to exchange interactions. They also proposed a new value, $L_{ij} = \sum_r (C_{ir}C_{jr})^2$, to estimate the mixing between the ith and the jth NBMOs, where C_{ir} is the coefficient of atomic orbital (AO) χ_r in the ith NBMO in the linear combination of AO (LCAO) approximation. Because one can consider unitary rotations between degenerated NBMOs, we define the L_{ij} value that provides the smallest value after the unitary transformation as $L_{ij}^{\min}$. The NBMO coefficients corresponding to the $L_{ij}^{\min}$ value are selected in order to minimize the mixing between the ith and jth NBMOs. The total energy difference between the excited singlet state and the excited triplet state at the Hartree−Fock MO level is expressed by using the exchange integral between the ith and jth NBMOs (K_{ij}) as $E(\mathrm{S}) - E(\mathrm{T}) = 2K_{ij}$, where E(S) and E(T) represent the total energy of the excited singlet state and the excited triplet state, respectively. The exchange integral K_{ij} is expressed as an MO-based two-electron integral $(rs|tu)$ by $K_{ij} = \sum_r \sum_s \sum_t \sum_u C_{ir}C_{js}C_{it}C_{ju}(rs|tu)$, where r, s, t, and u indicate AOs. Because the value of L_{ij} is proportional to the value of exchange integral K_{ij}, the high-spin stability of the system can be efficiently predicted by estimating the smallest $L_{ij}^{\min}$ value after unitary transformation.

Although the exchange interaction is closely related to the ferromagnetism of π-conjugated organic systems, little is known about the interaction path between radicals. The purpose of the present article is to elucidate the relationship between ferromagnetism and the interaction paths between radicals using through-space/bond (TS/TB) interaction analysis. From the analysis for benzyl radical species, it was found that TB interactions rather than TS interactions between radicals cause high-spin stability mainly in the electron correlation effects. In addition, we examined the dependency of high-spin stability on the size of a spacer between radicals. It was found that all-trans type TB interaction paths produce high-spin stability even when the size of the spacer is considerably large. It was also revealed that one could expect the high-spin stability that has

* Corresponding author e-mail: aoki@cube.kyushu-u.ac.jp.
[†] Kyushu University.
[‡] Hiroshima University.
[§] Group, PRESTO, Japan Science and Technology Agency (JST).

10.1021/jp060461s CCC: $33.50
Published on Web 03/31/2006

linear dependency on the number of radical units as long as we connect radical units with short-range TB interaction paths.

Methods

The concept of through-space (TS) and through-bond (TB) interactions has been widely used in various fields of chemistry[28−32] since Hoffmann et al. first proposed the concept.[33] TS/TB interaction analysis[34−39] was developed to analyze orbital interactions in a molecule quantitatively at the level of the ab initio MO method. We can estimate the contribution of specific orbital interactions to total energy by deleting the interactions in question. The deletion of the interaction between AOs χ_r that belongs to atom A and χ_s that belongs to atom B can be achieved by increasing the absolute magnitude of the exponents (α) in the Gaussian-type functions ($\exp(-\alpha r^2)$) of the basis functions corresponding to the interaction. If the exponents have a large limit ($\alpha \rightarrow \infty$), χ_r and χ_s are completely localized on each atomic nucleus. All the off-diagonal elements of the integrals between χ_r and χ_s lead to zero because of the disappearance of the orbital overlap.

The procedures for ab initio CI/MP TS/TB interaction analysis are summarized as follows (also see Figure 1 in ref 38):

(1) AO integrals are calculated using two types of basis functions, that is, normal basis functions with normal exponents (α) and artificial basis functions with extremely large exponents (α'). The AO integrals are stored separately in file 1 with the normal basis set and in file 2 with the artificial basis set.

(2) A new integrals file for TS/TB interaction analysis is obtained by merging file 1 and file 2. That is to say, integral elements related to "remaining" interactions are extracted from file 1 (normal basis set), whereas integral elements related to "deleting" interactions are extracted from file 2 (artificial basis set).

(3) Conventional Hartree−Fock self-consistent field (HF-SCF) calculations are performed using the new "merged" AO integrals file. This provides us with the total energy of the system after the specific orbital interactions are deleted.

(4) This treatment was enhanced to include the effects of electron correlations by linking with conventional configuration interaction (CI) and Møller−Plesset (MP) perturbation methods.

These procedures for the TS/TB interaction analysis were incorporated into program package GAMESS.[40] Except for the TS/TB analysis, all the ab initio calculations were performed using the Gaussian03 program package.[41]

Results and Discussion

Through-Space/Bond Interaction Analysis of Interaction Paths between Radicals. As shown in Figure 1(a), model **1** is a benzyl radical dimer model including a "0-∗ type" linkage. TS/TB interaction analysis was applied to model **1** to elucidate the relationship between the interaction paths and the high-spin stability of the system. The high-spin stability, ΔE(L−H), is defined as the difference in total energy between the lowest spin state (E(L)) and the highest spin state (E(H)), that is, ΔE(L−H) = E(L) − E(H). The positive value of ΔE(L−H) means that the high-spin state is more stable than the low-spin state. We use ΔE(S−T) for model **1**, which is expressed as the energy difference between the singlet and triplet states.

First, we calculated the electronic structure of model **1** in "full interaction (FULL)" state including all intramolecular interactions without any deletions. Open-shell systems are calculated using the restricted open-shell second-order MP (ROMP2) method. For the first step of the analysis, the singlet state was calculated as a closed-shell system. Single point

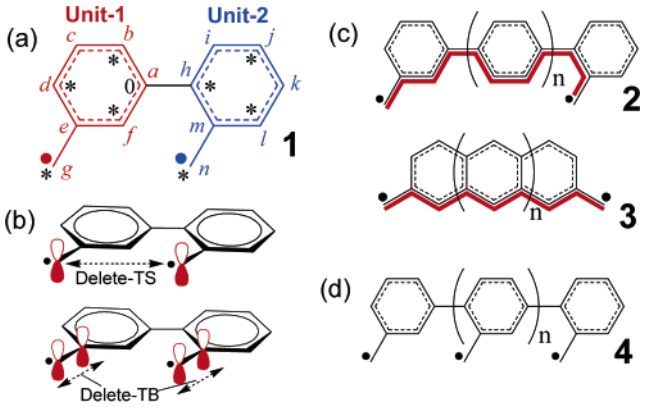

Figure 1. (a) Benzyl radical dimer model. Each radical unit is highlighted in red (unit 1) or blue (unit 2). Carbon sites $a-n$ are used for assigning the AOs in Figure 3. (b) Illustrations of the deletions of the through-space interaction path (delete-TS) and the through-bond interaction path (delete-TB) between radicals. (c) Models for examining spacer size dependency on high-spin stability. The "n" indicates the number of spacer units. The shortest TB interaction path is indicated by a red line. (d) Model for examining the dependency of the radical number on high-spin stability. The "$n + 2$" indicates the number of radicals.

TABLE 1: Through-Space/Bond Interaction Analysis of Interaction Paths between Radicals in Model 1 (ROMP2(FC)/6-311G//ROHF/6-311G)

	singlet	triplet	Δ^b (diff)
	(a) FULL (in au)		
$E_{total}{}^a$	−538.19131	−538.21364	0.02233
E_{HF}	−536.85608	−536.95551	0.09943
E_{corr}	−1.33523	−1.25812	−0.07711
	(b) Delete-TS^c (in au)		
$E_{total}{}^a$	−538.18914	−538.21363	0.02449
E_{HF}	−536.85406	−536.95551	0.10145
E_{corr}	−1.33508	−1.25812	−0.07696
	(c) Delete-TB^c (in au)		
$E_{total}{}^a$	−538.25594	−538.25868	0.00274
E_{HF}	−536.78541	−536.98574	0.20033
E_{corr}	−1.47052	−1.27293	−0.19759
	(d) Contribution of TB ("FULL" − "Delete-TB") (in au)		
$E_{total}{}^a$	0.06463	0.04504	0.01958
E_{HF}	−0.07066	0.03023	−0.10090
E_{corr}	0.13529	0.01481	0.12048

[a] E_{total} can be divided into Hartree−Fock (E_{HF}) and correlation (E_{corr}) energy terms, that is $E_{total} = E_{HF} + E_{corr}$. [b] The "Δ" represents the energy difference between the singlet and triplet states, that is, E(singlet state) − E(triplet state). [c] The deletions of through-space (TS) and through-bond (TB) interactions are illustrated in Figure 1(b).

calculations were performed at the level of ROMP2 (frozen core approximation (FC))/6-311G based on ROHF/6-311G optimized geometry under a fixed planar structure. We optimized the geometries of the singlet state and those of the triplet state independently. Triple valence functions such as a 6-311G basis set were adopted because p-orbitals that are perpendicular to the molecular plane should play an important role in π-conjugated systems. The whole high-spin stability ΔE_{total}(S−T) can be divided into Hartree−Fock energy term ΔE_{HF}(S−T) and electron correlations term ΔE_{corr}(S−T), which corresponds to the second-order perturbation energy, that is, ΔE_{total}(S−T) = ΔE_{HF}(S−T) + ΔE_{corr}(S−T). The results for the "FULL" state are shown in Table 1(a), and the schematic energy diagrams are shown in Figure 2 (left side). It was found that model **1** shows the high-spin stability of ΔE_{total}(S−T) with 0.022 au. The ΔE_{HF}(S−T) term provides high-spin stability with 0.099 au. In contrast, the ΔE_{corr}(S−T) term decreased the high-spin

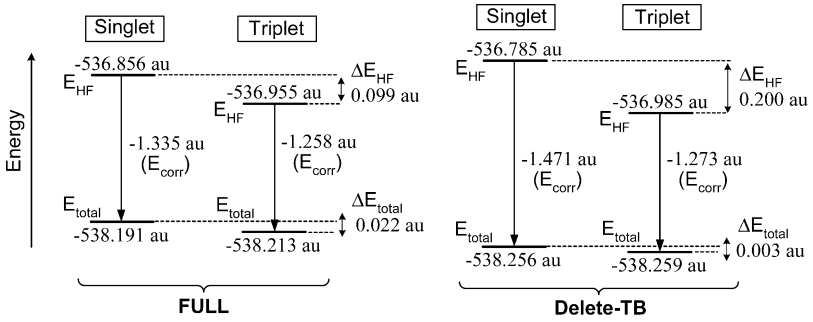

Figure 2. Schematic energy diagram for through-space/bond interaction analysis of model **1** (ROMP2(FC)/6-311G//ROHF/6-311G).

TABLE 2: HOMO-LUMO Component of Second-Order Perturbation Energy in the Singlet State of Model 1

	(i) $-\lvert[ia\rvert ia]\rvert^2$ (in au^2)	(ii) $2(\epsilon_a - \epsilon_i)$ (in au)	(iii) $-\lvert[ia\rvert ia]\rvert^2/2(\epsilon_a - \epsilon_i)$ (in au)
FULL	−0.00418	0.27232	−0.01534
delete-TB	−0.02197	0.22437	−0.09792
contribution of TB[a]			0.08258

[a] Difference between "FULL" and "delete-TB," i.e., "FULL" − "delete-TB."

stability by 0.077 au because the electron correlation term generally stabilizes the singlet state rather than the triplet state. As a result of the cancellation of the increase of ΔE_{HF}(S−T) and decrease of ΔE_{corr}(S−T), the high-spin stability ΔE_{total}(S−T) with 0.022 au remains.

Next, we deleted direct TS interaction between radical center carbon atoms at sites *g* and *n* by the TS/TB method, as shown in Figure 1(a),(b). We deleted all the interactions between p_z, p_z', and p_z'' on site *g* and those on site *n*, where the *Z*-axis is perpendicular to the molecular plane, and p_z, p_z', and p_z'' have different exponents. Deleting the TS interaction ("delete-TS" state) slightly changes the high-spin stability ΔE_{total}(S−T) from 0.022 to 0.024 au, as shown in Table 1(b). This means that direct TS interaction between radicals barely contributes to the high-spin stability of the system. The distance between the radical-center carbon atoms, 4.98 Å, in high-spin state geometry is far from the interaction through the overlap between the two radicals.

Finally, we eliminated TB interactions between radicals ("delete-TB" state) by deleting both p_z(site *e*)−p_z(site *g*) interaction and p_z(site *m*)−p_z(site *n*) interaction, as shown Figure 1(a),(b). As shown in Table 1(c) and Figure 2 (right side), it was found in "delete-TB" that ΔE_{total}(S−T) was considerably reduced from 0.022 (FULL) to 0.003 au. This means that around 88% of the high-spin stability comes from the TB interaction. However, the small stability in the ΔE_{total}(S−T) value with 0.003 au comes from the cancellation of the increase of ΔE_{HF}(S−T) by 0.200 au and the decrease of ΔE_{corr}(S−T) by 0.198 au. From Table 1(d), which shows the contribution of the TB interaction to the high-spin stability ΔE_{total}(S−T), we can point out the following items:

(1) The TB interaction contributes to ΔE_{total}(S−T) with 0.020 au. This contribution comes from the cancellation of the decrease of high-spin stability in ΔE_{HF}(S−T) by 0.101 au and the increase of high-spin stability in ΔE_{corr}(S−T) by 0.120 au.

(2) In Hartree−Fock energy terms, the decrease of ΔE_{HF}(S−T) dominantly comes from the large stabilization of the singlet state by 0.071 au.

(3) In correlation energy terms, the increase of ΔE_{corr}(S−T) by 0.120 au primarily results from the large destabilization of the singlet state by 0.135 au.

Therefore, the most important contribution of the TB interaction to the positive value of ΔE_{total}(S−T) is the singlet destabilization by 0.135 au in the electron correlation energy term.

We conducted a detailed analysis of the second-order perturbation energy (E_{corr}) in the singlet state of model **1** to examine the destabilization of the singlet state by the correlation effects. The HOMO−LUMO component of the second-order perturbation energy in the MP2 method can be expressed as

$$E_{corr}^{HOMO-LUMO} = -\frac{|[ia|ia]|^2}{2(\epsilon_a - \epsilon_i)} \quad (1)$$

where *i* and *a* indicate HOMO and LUMO, respectively (see also eq 6 of ref 37). The ϵ_i and ϵ_a represent orbital energies corresponding to HOMO (ϕ_i) and LUMO (ϕ_a), respectively. The MO-based two-electron integral is $[ia|ia] = \int \phi_i^*(1)\phi_a(1)(1/r_{12})\phi_i^*(2)\phi_a(2)d\tau_1 d\tau_2$. Table 2 shows the HOMO−LUMO component of E_{corr} in the singlet state for the "FULL" and "delete-TB" states, in which (i) the numerator of eq 1, $-|[ia|ia]|^2$, (ii) the denominator of eq 1, $2(\epsilon_a - \epsilon_i)$, and the (iii) whole component, $-|[ia|ia]|^2/2(\epsilon_a - \epsilon_i)$, is listed. It was found from the table that the deletion of the TB interaction considerably decreased the whole HOMO−LUMO component (iii) from −0.015 to −0.098 au. This result is due to both the increase of the absolute value of the numerator (from 0.004 to 0.022 au^2) and the decrease of the denominator (from 0.272 to 0.224 au). Figure 3(a),(b) shows MO coefficients corresponding to the HOMO and LUMO in the singlet state for the (a) FULL and (b) delete-TB states with their HOMO−LUMO energy gaps. The contribution of the TB interaction is summarized as follows from the "contribution of TB" in the same table and Figure 3(a),(b):

(1) The TB interaction contributes to the delocalization of HOMO and LUMO over the whole molecule using the π-network because these MOs are localized into radical center carbon atoms after the deletion of the TB interaction, as shown in Figure 3(b). The effect due to the TB interaction leads to the increase of the numerator $-|[ia|ia]|^2$, as seen in Table 2(i).

(2) The TB interaction increases the energy gap between HOMO and LUMO. This is confirmed in Figure 3 where the HOMO−LUMO gap is reduced by the deletion of the TB interaction from 0.136 to 0.112 au. The effect due to the TB interaction leads to an increase of the denominator $2(\epsilon_a - \epsilon_i)$, as shown in Table 2(ii).

The TB interaction destabilizes the whole HOMO−LUMO component of E_{corr} in the singlet state by 0.083 au, as shown in Table 2(iii). This energy change occupies around 61% of the destabilization of the perturbation term in the singlet state with 0.135 au, as mentioned before in Table 1(d). Therefore, the high-spin stability of model **1** results from the fact that the TB

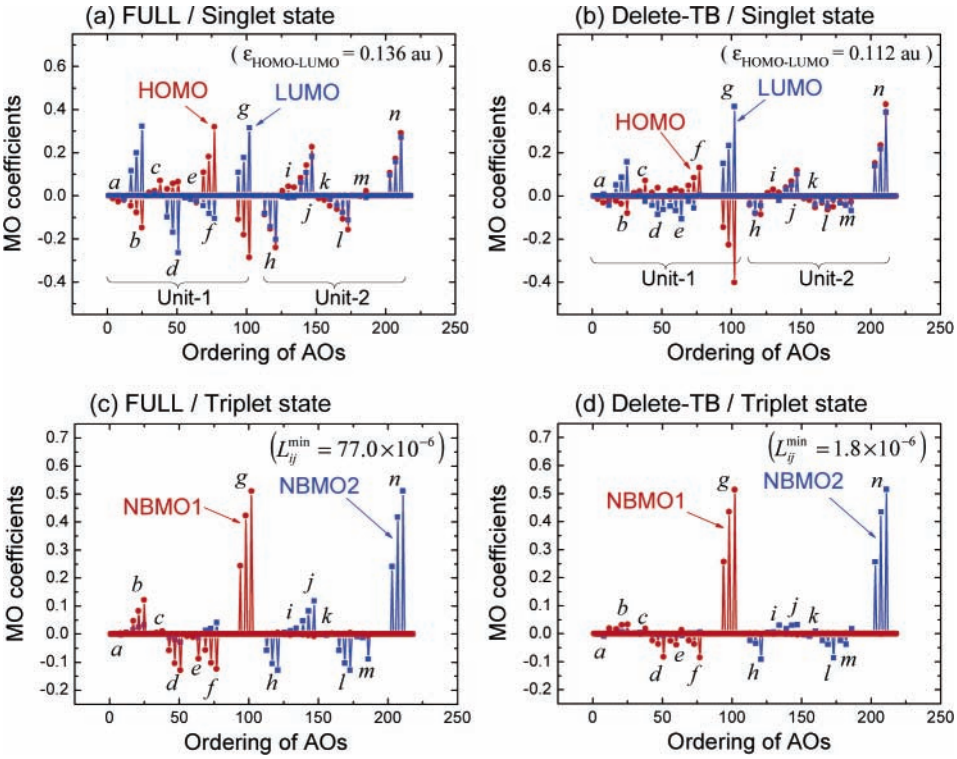

Figure 3. HOMO and LUMO in singlet state of model **1** for the (a) "FULL" and (b) "delete-TB" states. HOMO (red) and LUMO (blue) are shown in the same graph. The MO coefficients on each carbon site are assigned letters *a*−*n* according to Figure 1(a). The three peaks at each site correspond to the triple valence p_z, p_z', and p_z'' orbitals. The orbital energy gap between HOMO and LUMO ($\epsilon_{\mathrm{HOMO-LUMO}}$) is shown in parentheses. The NBMO coefficients correspond to the L_{ij}^{min} value after unitary rotations in the triplet state of model **1** for the (c) "FULL" and (d) "delete-TB" states. The two NBMOs are indicated in the same figure by different colors, that is, NBMO1 is red and NBMO2 is blue. The L_{ij}^{min} value is shown in parentheses.

interaction prevents the stabilization of the HOMO−LUMO component of the second-order perturbation energy in the singlet state.

Figure 3(c),(d) shows NBMO coefficients corresponding to the L_{ij}^{min} value for the (c) FULL and (d) delete-TB states in the high-spin state of model **1** to examine the validity of the L_{ij}^{min} value after unitary transformations. In the "FULL" state, both NBMO1 and NBMO2 have strong peaks of MO coefficients at the active carbon sites denoted by "∗" in Figure 1(a). Moreover, NBMO2, belonging to unit 2, is delocalized into the region of unit 1, while NBMO1 is not delocalized into the region of unit 2. We can confirm from panel (c) that the 0-∗ combination of two radical units results in a "nondisjoint" type linkage and produces the mixing between NBMOs. In the "delete-TB" state, shown in Figure 3(d), the peak strength of NBMO coefficients on radical center carbon atoms at sites *g* and *n* increases by ∼6% compared with the "FULL" state. The other NBMO coefficients on active carbon atoms denoted by *b*, *d*, *f*, *h*, *j*, and *l* decrease. That is, the feature of alternate hydrocarbons denoted by "0" and "∗" in NBMO is weakened by deleting the TB interaction. Moreover, the delocalization of NBMO2 into the region of unit 1 disappears considerably. Because each NBMO localizes into each radical unit, the localization makes the system more "disjointed". The change in the L_{ij}^{min} value from 77.0×10^{-6} ("FULL") to 1.8×10^{-6} ("delete-TB") also exhibits the decrease of NBMO mixings by deleting the TB interactions. In other words, the TB interaction enhances the delocalization of NBMOs and makes the system more "nondisjointed". Although the detailed analyses of the perturbation energy in the singlet state as mentioned before and the L_{ij}^{min} value estimated by the high-spin state are totally different approaches to high-spin stability, they show a similar tendency for the deletion of the TB interactions. It was therefore concluded that one could make reasonable predictions of high-spin stability by using the L_{ij}^{min} value.

Dependence of High-Spin Stability on Spacer Size and Number of Radicals. In the previous subsection, it was found that the TB interaction between radicals produces high-spin stability in relation to the electron correlation effects. In this subsection, we examine the dependence of high-spin stability on spacer size and number of radicals from the point of view of the TB interaction path between radicals.

First, we examine the relationship between spacer size and high-spin stability, $\Delta E_{\mathrm{total}}(\mathrm{S-T})$, for models **2** and **3** in Figure 1(c), where the number of spacer units is specified by "*n*". Single-point calculations were performed by ROMP2(FC)/6-311G on the ROHF/6-311G fully optimized geometry in the framework of planar structures. Model **3** involves an all-trans TB interaction path between radicals indicated by a red line, whereas model **2** includes cis-type pathways in the TB interaction path. The results for models **2** and **3** are shown in Figure 4 (parts a and b, respectively). The electron correlation terms are also shown in panel (d) for model **2** and panel (e) for model **3**, where the whole high-spin stability $\Delta E_{\mathrm{total}}(\mathrm{S-T})$ can be divided into $\Delta E_{\mathrm{HF}}(\mathrm{S-T})$ and $\Delta E_{\mathrm{corr}}(\mathrm{S-T})$.

In model **2**, $\Delta E_{\mathrm{total}}(\mathrm{S-T})$ abruptly decreases as the number of spacer units (*n*) increases, as seen in panel (a). Even when $n = 2$, $\Delta E_{\mathrm{total}}(\mathrm{S-T})$ exhibits a negative value, that is, low-spin stability. This effect results from the drastic reduction of $\Delta E_{\mathrm{corr}}(\mathrm{S-T})$, while $\Delta E_{\mathrm{HF}}(\mathrm{S-T})$ gradually increases as *n* increases, converging to a nearly constant value. As seen in panel (d), the correlation energy term $\Delta E_{\mathrm{corr}}(\mathrm{S-T})$ of model **2** indicates that the singlet state is rapidly stabilized with *n* increases compared with the triplet state. In model **3**, panel (b) shows that $\Delta E_{\mathrm{total}}(\mathrm{S-T})$ gradually decreases as *n* increases. This is because ΔE_{HF}-

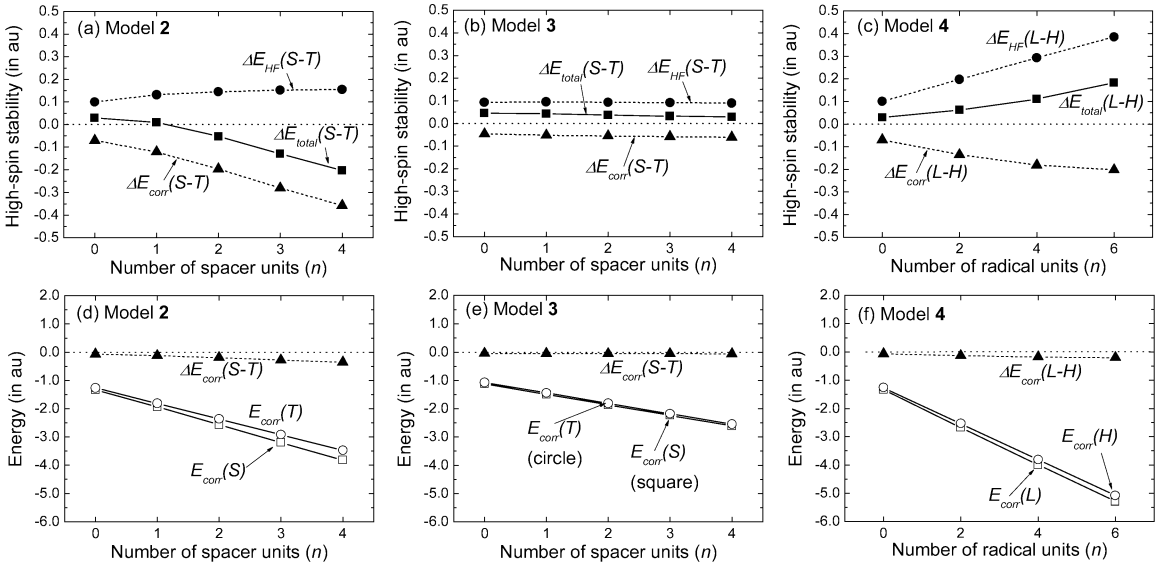

Figure 4. Dependence of high-spin stability on spacer size or number of radical units for (a) models **2**, (b) **3**, and (c) **4** by ROMP2(FC)/6-311G//ROHF/6-311G. (d)−(f) show the changes in terms of correlation energy by second-order perturbation energy using the MP2 method. In model **4**, only the even-number n is selected, and the total number of radicals becomes even-number $n + 2$. For model **4**, low-spin means the singlet state, and the high-spin state is treated as the highest spin state.

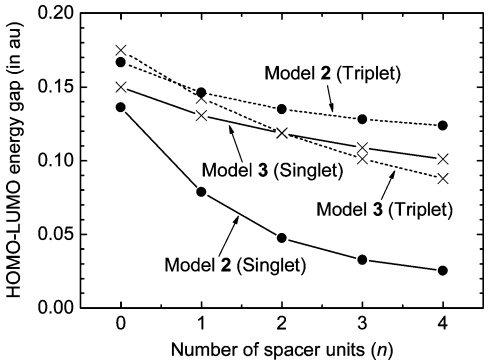

Figure 5. Spacer size dependency of the HOMO−LUMO energy gap for model **2** (closed-circle) and model **3** (cross). The solid and broken lines indicate the singlet and triplet states, respectively. In the triplet state, the energy gap between the highest NBMO and LUMO is plotted.

(S−T) maintains a constant value, while ΔE_{corr}(S−T) decreases very slowly. Therefore, we can expect long-range exchange interactions between radicals in model **3** including the all-trans TB interaction path. As seen in panel (e), ΔE_{corr}(S−T) of model **3** shows that both the singlet and triplet states decrease at nearly the same speed.

From these results, it was found that the high-spin stability of the system is dominantly controlled by the behavior of the electron correlation term rather than the Hartree−Fock energy term. In particular, the difference in energy between the singlet and triplet states is more important rather than the absolute value of the correlation energy. The different behaviors of ΔE_{corr}(S−T) in models **2** and **3** can be explained qualitatively by the HOMO−LUMO energy gap. Figure 5 shows the spacer size dependency of the HOMO−LUMO energy gap for models **2** and **3**. The energy gap between the highest NBMO and LUMO is plotted for the triplet state. In model **2**, the spacer size dependency of the energy gap shows a different tendency between the singlet and triplet states. Compared with the triplet state, the singlet state largely reduces the energy gap with n increases. This means that in the singlet state of model **2** the absolute value of the HOMO−LUMO component of the perturbation energy in eq 1 increases remarkably with an increase of n because the denominator $2(\epsilon_a - \epsilon_i)$ of eq 1 decreases. It is obvious from the graph that the difference in the energy gap converges to a constant value at a large n. Therefore, the numerator $-|[ia|ia]|^2$ of eq 1 plays a dominant role in the behavior of ΔE_{corr}(S−T) at a larger n. In contrast, in model **3** the behavior of the energy gap is very similar regardless of the multiplicity. This result explains the fact that the E_{corr}(S) and E_{corr}(T) show a similar tendency to decrease in panel (e) by considering the energy gap part of the second-order perturbation energy.

Finally, we examined the dependency of the high-spin stability of model **4** shown in Figure 1(d) on the number of radical units. Even numbers of center units $n = 0$, 2, 4, and 6 were selected for model **4**. However, we should note that the total number of the radicals is $n + 2 = 2$, 4, 6, and 8. In model **4**, the low-spin state means the singlet state, and the high-spin state is treated as the highest spin state. For example, the quintet state is applied for the high-spin state of the model with the number of radicals $n + 2 = 4$. As seen in Figure 4(c), ΔE_{total}(L−H) increases in proportion to the number of radicals (n). This result is caused by the increase of ΔE_{HF}(L−H) in proportion to n and the fact that the change in ΔE_{corr}(L−H) converges to a constant value. Figure 4(f) shows the correlation energy term for model **4**. In the correlation energy term, the stabilization of the low-spin state is larger than that of the high-spin state. However, both states decrease with nearly the same increment as n increases, leading to the constant value of ΔE_{corr}(L−H). Therefore, we can expect the high-spin stability in which the stabilization energy increases linearly with the number of radicals as long as the radical units are connected while keeping the short-range TB interaction path.

Conclusion

Interaction path analyses were performed to examine the relationship between the orbital interaction between radicals and ferromagnetic properties in π-conjugated organic systems. It was found that the high-spin stability of the benzyl radical species primarily results from the TB interaction between radicals. The TB interaction prevents the stabilization of the low-spin state energy caused by electron correlation effects, leading to stabilization in the high-spin state in some systems. The TB

interaction also makes the system more "nondisjointed" due to the delocalization of NBMOs. It was confirmed that the relationship between the TB interactions and the high-spin stability was well predicted by $L_{ij}^{\min}$ value for estimating the NBMO mixings. In contrast with the TB interaction, TS interaction between radicals does not contribute to the high-spin stability of the system. Furthermore, it was found that long-range exchange interaction is expected in the systems with an all-trans type interaction path between radicals, and the additivity of the high-spin stability for the number of radicals can be achieved as long as radical units are connected while keeping the short-range interaction path. The long-range exchange interactions and the additivity of high-spin stability are primarily controlled by the electron correlation effects.

Acknowledgment. This work was supported by a grant-in-aid from the Ministry of Education, Culture, Sports, Science and Technology of Japan (MEXT) and by the Research and Development for Applying Advanced Computational Science and Technology of the Japan Science and Technology Agency (ACT-JST). The calculations were performed on the Linux PC clusters in our laboratory.

References and Notes

(1) Fujita, W.; Awaga, K. *Science* **1999**, *286*, 261−262.
(2) *Molecular Magnetism*; Ito, K., Kinoshita, M., Eds.; Kodansha, Gordon and Breach: Tokyo and Amsterdam, 2000.
(3) Rajca, A. *Chem. Rev.* **1994**, *94*, 871−893.
(4) Rajca, A.; Wongsriratanakul, J.; Rajca, S.; Cerny, R. *Angew. Chem., Int. Ed.* **1998**, *37*, 1229−1232.
(5) Rajca, A.; Rajca, S.; Wongsriratanakul, J. *J. Am. Chem. Soc.* **1999**, *121*, 6308−6309.
(6) Rajca, A. *Chem. Eur. J.* **2002**, *8*, 4834−4841.
(7) Rajca, A.; Wongsriratanakul, J.; Rajca, S.; Cerny, R. L. *Chem. Eur. J.* **2004**, *10*, 3144−3157.
(8) Rajca, A.; Wongsriratanakul, J.; Rajca, S. *J. Am. Chem. Soc.* **2004**, *126*, 6608−6626.
(9) Rajca, S.; Rajca, A.; Wongsriratanakul, J.; Butler, P.; Choi, S. *J. Am. Chem. Soc.* **2004**, *126*, 6972−6986.
(10) Rajca, A.; Wongsriratanakul, J.; Rajca, S. *Science* **2001**, *294*, 1503−1505.
(11) *Magnetic Properties of Organic Materials*; Lahti, P. M., Ed.; Marcel Dekker: New York, 1999.
(12) Nishide, H.; Miyasaka, M.; Tsuchida, E. *Angew. Chem., Int. Ed. Engl.* **1998**, *37*, 2400−2402.
(13) Miyasaka, M.; Yamazaki, T.; Tsuchida, E.; Nishide, H. *Macromolecules* **2000**, *33*, 8211−8217.
(14) Sato, K.; Shimoi, D.; Takui, T.; Hattori, M.; Hirai, K.; Tomioka, H. *Synth. Met.* **2001**, *121*, 1816−1817.
(15) Oda, N.; Nakai, T.; Sato, K.; Shimoi, D.; Kozaki, M.; Okada, K.; Takui, T. *Synth. Met.* **2001**, *121*, 1840−1841.
(16) Michinobu, T.; Inui, J.; Nishide, H. *Org. Lett.* **2003**, *5*, 2165−2168.
(17) Fukuzaki, E.; Nishide, H. *J. Am. Chem. Soc.* **2006**, *128*, 996−1001.
(18) Pranata, J. *J. Am. Chem. Soc.* **1992**, *114*, 10537−10541.
(19) Mitani, M.; Mori, H.; Takano, Y.; Yamaki, D.; Yoshioka, Y.; Yamaguchi, K. *J. Chem. Phys.* **2000**, *113*, 4035−4051.
(20) Dietz, F.; Tyutyulkov, N. *Chem. Phys.* **2001**, *264*, 37−51.
(21) Huai, P.; Shimoi, Y.; Abe, S. *Phys. Rev. Lett.* **2003**, *90*, 207203.
(22) Dias, J. R. *J. Chem. Inf. Comput. Sci.* **2003**, *43*, 1494−1501.
(23) Hagiri, I.; Takahashi, N.; Takeda, K. *J. Phys. Chem. A* **2004**, *108*, 2290−2304.
(24) Borden, W. T.; Davidson, E. R. *J. Am. Chem. Soc.* **1977**, *99*, 4587−4594.
(25) Borden, W. T. *Mol. Cryst. Liq. Cryst.* **1993**, *232*, 195−218.
(26) Fang, S.; Lee, M.-S.; Hrovat, D. A.; Borden, W. T. *J. Am. Chem. Soc.* **1995**, *117*, 6727−6731.
(27) Aoki, Y.; Imamura, A. *Int. J. Quantum Chem.* **1999**, *74*, 491−502.
(28) Post, A. J.; Nash, J. J.; Love, D. E.; Jordan, K. D.; Morrison, H. *J. Am. Chem. Soc.* **1995**, *117*, 4930−4935.
(29) Lange, H.; Schafer, W.; Gleiter, R.; Camps, P.; Vazquez, S. *J. Org. Chem.* **1998**, *63*, 3478−3480.
(30) Gineityte, V. *J. Mol. Struct. (THEOCHEM)* **1998**, *430*, 97−104.
(31) Mackenzie-Ross, H.; Brunger, M. J.; Wang, F.; Adcock, W.; Trout, N.; McCarthy, I. E.; Winkler, D. A. *J. Electron Spectrosc. Relat. Phenom.* **2002**, *123*, 389−395.
(32) de Visser, S. P.; Filatov, M.; Schreiner, P. R.; Shaik, S. *Eur. J. Org. Chem.* **2003**, 4199−4204.
(33) Hoffmann, R.; Imamura, A.; Hehre, W. J. *J. Am. Chem. Soc.* **1968**, *90*, 1499−1509.
(34) Imamura, A.; Sugiyama, H.; Orimoto, Y.; Aoki, Y. *Int. J. Quantum Chem.* **1999**, *74*, 761−768.
(35) Orimoto, Y.; Aoki, Y. *Int. J. Quantum Chem.* **2002**, *86*, 456−467.
(36) Orimoto, Y.; Aoki, Y. *Int. J. Quantum Chem.* **2003**, *92*, 355−366.
(37) Orimoto, Y.; Aoki, Y. *Phys. Rev. A* **2003**, *68*, 063808 1−6.
(38) Orimoto, Y.; Naka, K.; Takeda, K.; Aoki, Y. *Org. Biomol. Chem.* **2005**, *3*, 2244−2249.
(39) Orimoto, Y.; Naka, K.; Aoki, Y. *Int. J. Quantum Chem.* **2005**, *104*, 911−918.
(40) GAMESS. Schmidt, M. W.; Baldridge, K. K.; Boatz, J. A.; Elbert, S. T.; Gordon, M. S.; Jensen, J. H.; Koseki, S.; Matsunaga, N.; Nguyen, K. A.; Su, S. J.; Windus, T. L.; Dupuis, M.; Montgomery, J. A. *J. Comput. Chem.* **1993**, *14*, 1347−1363.
(41) Frisch, M. J.; Trucks, G. W.; Schlegel, H. B.; Scuseria, G. E.; Robb, M. A.; Cheeseman, J. R.; Montgomery, J. A., Jr.; Vreven, T.; Kudin, K. N.; Burant, J. C.; Millam, J. M.; Iyengar, S. S.; Tomasi, J.; Barone, V.; Mennucci, B.; Cossi, M.; Scalmani, G.; Rega, N.; Petersson, G. A.; Nakatsuji, H.; Hada, M.; Ehara, M.; Toyota, K.; Fukuda, R.; Hasegawa, J.; Ishida, M.; Nakajima, T.; Honda, Y.; Kitao, O.; Nakai, H.; Klene, M.; Li, X.; Knox, J. E.; Hratchian, H. P.; Cross, J. B.; Adamo, C.; Jaramillo, J.; Gomperts, R.; Stratmann, R. E.; Yazyev, O.; Austin, A. J.; Cammi, R.; Pomelli, C.; Ochterski, J. W.; Ayala, P. Y.; Morokuma, K.; Voth, G. A.; Salvador, P.; Dannenberg, J. J.; Zakrzewski, V. G.; Dapprich, S.; Daniels, A. D.; Strain, M. C.; Farkas, O.; Malick, D. K.; Rabuck, A. D.; Raghavachari, K.; Foresman, J. B.; Ortiz, J. V.; Cui, Q.; Baboul, A. G.; Clifford, S.; Cioslowski, J.; Stefanov, B. B.; Liu, G.; Liashenko, A.; Piskorz, P.; Komaromi, I.; Martin, R. L.; Fox, D. J.; Keith, T.; Al-Laham, M. A.; Peng, C. Y.; Nanayakkara, A.; Challacombe, M.; Gill, P. M. W.; Johnson, B.; Chen, W.; Wong, M. W.; Gonzalez, C.; Pople, J. A. *Gaussian 03, Revision C.02*; Gaussian, Inc.: Wallingford, CT, 2004.